

The role of pressure-induced stacking faults on the magnetic properties of gadolinium

Rafael Martinho Vieira,^{1,2} Olle Eriksson,¹ Torbjörn Björkman,² Ondřej Šipr,^{3,4} and Heike C. Herper¹

¹*Department of Physics and Astronomy,
Uppsala University, Box 516, SE-751 20 Uppsala, Sweden*

²*Physics, Faculty of Science and Engineering,
Åbo Akademi University, FI-20500 Turku, Finland*

³*FZU–Institute of Physics of the Czech Academy of Sciences,
Cukrovarnická 10, CZ-160 00 Prague, Czech Republic*

⁴*New Technologies Research Centre,
University of West Bohemia, CZ-301 00 Pilsen, Czech Republic*

(Dated: September 6, 2023)

Abstract

Experimental data show that under pressure, Gd goes through a series of structural transitions $hcp \rightarrow Sm\text{-type (close-packed rhombohedral)} \rightarrow dhcp$ that is accompanied by a gradual decrease of the Curie temperature and magnetization till the collapse of a finite magnetization close to the $dhcp$ structure. We explore theoretically the pressure-induced changes of the magnetic properties, by describing these structural transitions as the formation of fcc stackings faults. Using this approach, we are able to describe correctly the variation of the Curie temperature with pressure, in contrast to a static structural model using the hcp structure.

I. INTRODUCTION

Being the elemental metal with the highest known atomic spin moment at low temperature, Gd seized early the attention of the magnetism community, and its properties are very well documented [1, 2]. Several studies of its magnetic, structural and spectroscopic properties have been reported, from experiments and theory. Within the existing literature on first-principles calculations for Gd, it is possible to find different treatments of the f -states and their respective impact on the electronic band structure [3, 4]. In conjunction with other studies on magnetic properties such as magnetic moment [5, 6], the exchange parameters [3, 4], magnetic anisotropy [7] and magnetic entropy [8], they have proven to be critical for the description of the fundamental magnetic phenomena and establish a solid background on the capabilities and limitations of ab-initio methods in studying Gd.

Recently, there has been a discussion of the magnetic properties of Gd under pressure [9–12]. Experiments report a gradual decrease in the magnetization and the Curie temperature till around 6 GPa, where the magnetization collapses [10, 11, 13–17], attributing generally such collapse to a shift in the magnetic ordering from

ferromagnetic (FM) to antiferromagnetic (AFM).

Accompanying the changes in the magnetic properties in Gd under pressure, there are also changes in the crystal structure. At around 2 GPa the structure is reported to go from hexagonal-closed-packed (*hcp*) to a *Sm*-type structure (*9R*) and then at 6.5 GPa, close to where the magnetization collapses, there is a structural transformation to a double-hexagonal-close-packed structure (*dhcp*). The coupling between the magnetic and structural properties has not been investigated in detail, which is the motivation behind the present investigation.

In this work, we show that pure volumetric effects alone do not explain the pressure-induced variations of the magnetic properties. This is in agreement with a previous theoretical study [9], which found a strong coupling between the stability of the high-pressure structures and the magnetic properties. This work implied that structural changes along the transformation path $hcp \rightarrow Sm\text{-type } (9R) \rightarrow dhcp$ strongly impact the magnetic properties. In this work, we elucidate this finding by means of ab-initio electronic structure theory, coupled with atomistic spin simulations.

The *dhcp*, *hcp*, and *9R* structures are hexagonal stacked structures that result from a repeating pattern of A, B, and C stacked hexagonal layers with slightly different arrangements of atoms. Depending on the arrangement of these layers, either face-centred cubic, *fcc*, (ABCABC...) or *hcp* (ABAB...) environments are formed. For example, the *hcp* structure (ABAB) contains only sites with *hcp* environments, while the *9R* structure (ABABCBCAC) comprises six sites with a *hcp* environment and three sites with a *fcc* environment. In the *dhcp* structure (ABAC), there exist two sites with a *hcp* environment and two others with a *fcc* environment.

Since these structures differ primarily in the ratio of *hcp-fcc* environments, one can describe the observed, pressure-induced transformation from *hcp* to *Sm*-type to the *dhcp* structure as the formation/accumulation of *fcc* periodic stacking fault

structures [18]. This picture is compatible with experiment [19]: e.g., the equation of state does not exhibit any drastic variation of the volume or elastic properties at the transition pressures, indicating their second-order nature. In addition, it allows for a simplified model of the structural changes and reformulates the problem in terms of a relationship between the magnetic properties of Gd and the presence of *fcc* stacking faults. In the following, we explore this possibility to explain the observed pressure dependence of the magnetization and Curie temperature.

II. MATERIALS AND METHODS

A. Computational details

Density functional theory (DFT) calculations of the magnetic and electronic structure were made using the RSPt code [20], a full-potential linear muffin-tin orbitals method. Calculations are performed within the local spin density approximation (LSDA) [21] and the *f*-electrons are treated as spin-polarized core states (open-core approximation). This setup has been shown to avoid artificial hybridization of *f*-states with *d*-electrons seen in simple DFT calculations of *hcp* Gd [3]. Moreover, in Ref. [9], it was observed that the treatment of *f*-electrons does not play a role in structural stability, so we found it reasonable to use the same setup for the *Sm*-type and the *dhcp* structures. The package *cif2cell* was used in the preparation of the DFT input files [22].

To compare the energies of various magnetic configurations, including those with magnetic disorder in *fcc* sites, additional calculations were performed using the KKR method [23, 24] as implemented in SPR-KKR method [25]. The magnetic disorder was modelled using the disordered local moments (DLM) approach and treated using the coherent potential approximation (CPA) [26, 27]. For this set of calculations,

f -states were treated within the LSDA+U correction in the rotationally invariant formulation [28] with an $U=6.7$ eV and $J=0.7$ eV [4].

Using the RSPt software we calculated the Heisenberg exchange couplings, J_{ij} , within the LKAG formalism [29, 30], which we used as input for Monte Carlo (MC) simulations performed within the UppASD code [31, 32] in order to capture the temperature effects of the magnetic properties. In the MC simulations, we made use of the conventional atomistic Heisenberg Hamiltonian:

$$\mathcal{H} = -\frac{1}{2} \sum_{i \neq j} J_{ij} \mathbf{e}_i \cdot \mathbf{e}_j - \sum_i \mathbf{H} \cdot \mathbf{m}_i, \quad (1)$$

which describes the pair exchange interactions between magnetic moments (\mathbf{m}) pointing along unit vectors (\mathbf{e}), and the interaction of the magnetic moments with an external magnetic field (\mathbf{H}). The MC simulations were performed for the *hcp* as described in Ref. [8], while for the *dhcp* and *Sm*-type phases, we considered a simulation box with a minimum of approximately ≈ 83000 sites and 75000 MC steps with the Metropolis algorithm.

B. Model structures

Whereas the *hcp* phase of Gd is known to have a ferromagnetic (FM) ordering, the *Sm*-type and *dhcp* phases have been suggested to be antiferromagnetically (AFM) ordered between pairs of the hexagonal planes (A-type AFM) [9, 10]. Hence, we compared the ground-state energies and magnetic properties of the FM/AFM configurations for the structures under pressure.

The AFM configuration is incommensurate with the *Sm*-type structure, becoming non-trivial in how the moments in *fcc*-environment sites are aligned. They either become magnetically frustrated [10] or one has to consider a magnetic unit cell that is twice the structural unit cell, to achieve a lattice that has a proper periodicity of the

structure and magnetic properties. We explored the stability of these possible AFM arrangements (see Figure 1) in the DFT calculations. Additionally, we included a ferrimagnetic-like (FiM) configuration, where magnetic moments at the fcc sites have all the same orientation and can be seen as an AFM state with a magnetic defect (caused by the magnetic frustration).

The lattice parameters of the structures considered and magnetic moments resultant from the FP-LMTO calculations at ambient conditions, are summarized in Table I. As in other calculations [9], we observe only a tiny variation in the local magnetic moments when different magnetic and structural arrangements are considered. In the case of the Sm -type structure, we observe in Table I that the AFM state with a doubled structural unit cell has the lowest energy of all arrangements considered in FP-LMTO calculations (see Table S.II in Supplement). This is consistent with previous findings [9]. However, the very similar energy of the FiM state shows that low-lying, possibly non-collective magnetic excitations are possible for this polymorph. In the KKR-CPA calculations, the ground state is found to be FM instead, but we observe similar energies for the AFM and FiM states. More importantly, we observe that magnetic frustration in the fcc sites (with DLM moments) is not energetically favourable for both FM or AFM configurations.

For the $dhcp$ structure, we see (see Supplement) that the DFT energies differ from other works, which predict this phase to be AFM [9]. We observe instead that the FM state has lower energy. However, atomistic Monte Carlo simulations using the exchange parameters obtained from the ferromagnetic configuration of the electronic structure calculations, result in a complex magnetic configuration. These results will be presented in the following section.

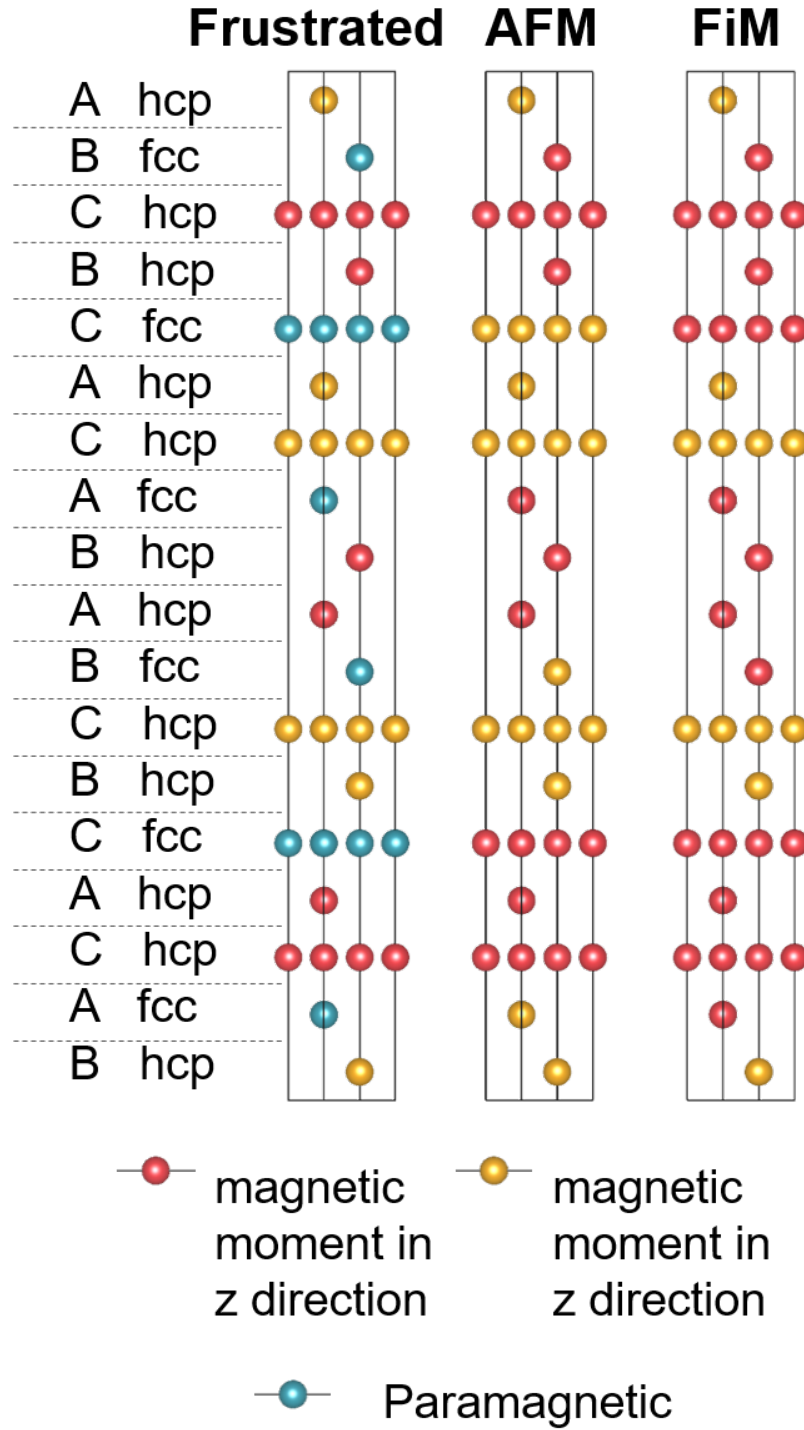


FIG. 1. Schematic picture of the setup considered for different magnetic configurations (AFM and FiM) of Gd in the Sm -type structure.

Phase	a (Å)	c/a	$\langle m_{site} \rangle$ (μ_B)	ΔE_0 (mRy/atom)
<i>hcp</i> (FM)	3.642 [8]	1.60	7.59	-
<i>Sm</i> -type				
AFM			7.49	0
FiM	3.618 [33]	14.43	7.49	0.02
FM			7.53	0.31
<i>dhcp</i>				
FM			7.41	0
AFM	3.402 [34]	3.25	7.37	0.39

TABLE I. Summary of the structural and magnetic properties from the DFT (FP-LMTO) calculations at ambient conditions.

III. RESULTS AND DISCUSSION

A. Exchange parameters

The exchange parameters (J_{ij}) of the three investigated structures (*hcp*, *Sm*-type, *dhcp*) obtained for the respective magnetic DFT ground state configuration are given in Figure 2. These values serve as input for the subsequent Monte Carlo simulations. The J_{ij} values show similarities between phases, with the most significant disparity being the presence of strong long-range AFM couplings in the region $1.7 < d/a < 2.0$ for the *Sm*-type and *dhcp* phases. Such couplings are likely responsible for destabilizing a pure FM order in these structures under pressure. A similar increase in the strength of AFM exchange is observed for elemental Nd when comparing the *dhcp* phase against the *hcp* structure [35], which was argued to be responsible for the self-induced spin-glass state of this system.

In general, for the *dhcp* and *Sm*-type structure, we observe that coupling between first neighbours that appear between an fcc site and an hcp site is weaker than couplings between atoms that both are at hcp sites. Furthermore, we observe in all phases the oscillatory behaviour of the J_{ij} that characterizes RKKY interactions. The frequency of these oscillations is smaller in the *dhcp* phase compared to the *Sm*-type and *hcp* phases (see Figure 2b). In Ref. [15] it is pointed out that the reduction of the lattice parameter by pressure will lower the bottom of the conduction band leading to a decrease in the density of states at the Fermi level ($D(\epsilon_F)$). Since the strength of RKKY interactions is proportional to $D(\epsilon_F)$ [15], this would lead to the decrease of exchange interactions and hence to a lower T_C . In our first-principles calculations for compressed volumes of the *hcp* structure (see Table III in the Supplement), we do indeed observe a reduction of the $D(\epsilon_F)$ that is accompanied by a decrease of the T_C (e.g as calculated from mean-field theory, see blue circles in Figure 3). However, as this figure shows, the pressure dependence of the theoretical values is significantly less pronounced than in the experiment. Additionally, for higher pressures, between 4 GPa and 6 GPa, $D(\epsilon_F)$ increases with the volume reductions, due to intricate details of the electronic structure, while the respective calculation for T_C decreases. This implies that the variation of the RKKY interactions solely by volumetric effects does not explain the observed experimental trend for T_C .

An interesting aspect is that we observe a significant increase in the strength of the 1st and 2nd nearest neighbours' exchange interactions (FM) between atoms in *hcp*-like environments for the *Sm*-type structure in comparison to the *hcp* structure. This result seems counter-intuitive since the experimental trend for T_C with pressure ($dT_C/dP < 0$) would suggest that the decrease of T_C is a consequence of the weakening of the ferromagnetic couplings. We observe that instead, an increase in AFM couplings is responsible for the decrease in the ordering temperature, see Figure 2. Nevertheless, this set of exchange parameters allows us to determine an

order-disorder transition temperature close to experimental observations.

B. Monte Carlo simulations

Materials with comparable FM and AFM couplings tend to develop more complex magnetic configurations, such as spin spirals or spin glasses, in order to balance these competing alignments [35]. For simplicity, we assume collinear configurations in the DFT calculation. However, the J_{ij} parameters calculated for these configurations should capture this competition between FM-AFM couplings and can therefore be used in MC simulations to get a more realistic picture of the magnetic configuration. This analysis is particularly interesting for the *Sm*-type and *dhcp* structures due to the significant AFM couplings which resulted from these calculations, see Figure 2.

Experimentally, a finite magnetization is measured for the *Sm*-type phase, which is not in agreement with the AFM configuration predicted by the theory reported in Table 1. However, if there is some non-collinearity (e.g. magnetic canting), a finite magnetization can arise in the AFM configuration. A finite magnetic moment can also occur if an external magnetic field is present or due to finite temperature effects which might stabilize a FM configuration over an AFM ordering. Also, if the *hcp* and *Sm*-type phases coexist, the *Sm*-type phase will experience the magnetization of the *hcp* phase as an external magnetic field, and hence obtain a finite magnetization. This induced field could, in a very simple model, be included in the interaction between the two magnetic subsystems.

For this reason, we considered two possible setups in the Monte Carlo simulations. First, we simulated a field-free relaxation, guided only by the exchange parameters corresponding to the pure *Sm*-type phase. Afterwards, we proceeded with a MC relaxation under a magnetic field of 2.75T, which is the magnitude of the magnetic field generated by the ordered moments in the *hcp* phase, to describe the case of

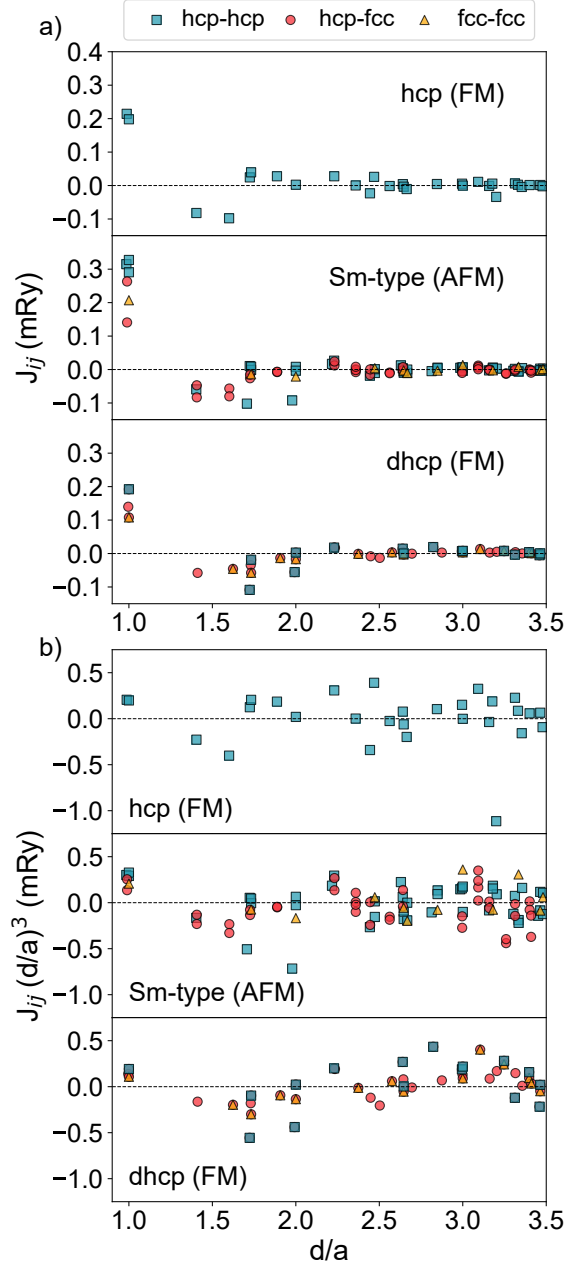


FIG. 2. a) Exchange parameters for Gd in the *hcp* (top), *Sm*-type (middle) and *dhcp* (bottom) structures obtained from the respective ground states according to DFT calculations. b) Equivalent to a) with a prefactor $(d/a)^3$ on the exchange parameters, to highlight the RKKY interaction. The interaction between different types of sites in the stacking sequence is given as *hcp-hcp*, *hcp-fcc* and *fcc-fcc*.

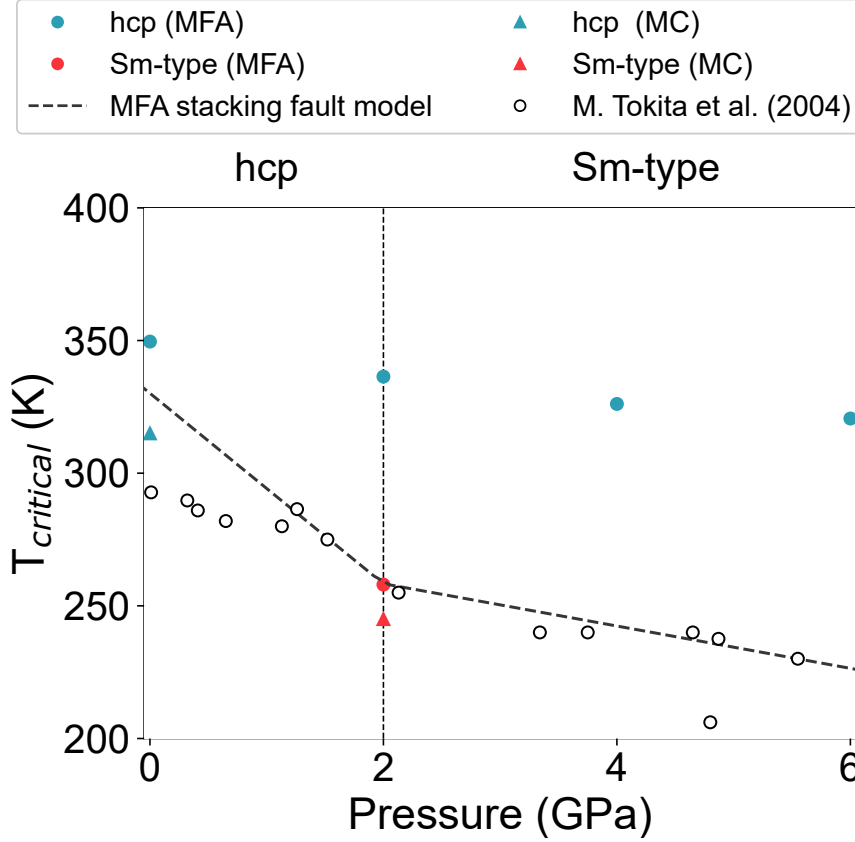


FIG. 3. Curie temperature variation with pressure. Open circles refer to experimental data extracted from Ref. [15], while filled circles are mean-field approximations of T_C from the ab-initio exchange parameters. The triangles correspond to the critical temperature calculated from the Monte Carlo simulations. A solid line is used for the mixing model for *hcp* and *fcc* stacks to estimate T_C (for more details we refer to the text).

coexistence of *hcp* and *Sm-type* phases, with the latter embedded in the former. Applying an external field is also more realistic for comparison of the calculated magnetization to measurements later.

In the field-free simulation, no finite magnetization is obtained in the *Sm-type* phase in the temperature range of 1 to 300 K. The spin distribution shown in Fig-

ure 4a appears to be roughly an AFM configuration with some degree of disorder but with a clear general orientation of spins. In contrast to that, the setup with applied external magnetic field results in a configuration with a magnetization of roughly $1 \mu_B$ per atom (Fig. 4b). The magnetic field breaks the symmetry, giving rise to a finite induced magnetic moment, while simultaneously increasing the spin disorder in the perpendicular plane, see Fig. 4b. The calculated heat capacity (see Figure S.?? in Supplement) in the simulation range of 1 to 300 K, reveals that both sets of calculations have critical temperatures of around 245 K. Both setups also share a smaller peak on the heat capacity of around 100K. This smaller peak suggests that there is a new magnetic regime likely to be caused by temperature fluctuations overcoming one (or a set of) significant exchange couplings.

A further increase of the pressure leads to the collapse of a magnetically ordered state with finite magnetization and then a transition to the *dhcp* phase. In this phase, we observed that although the DFT energies for the *dhcp* phase predict a FM configuration, the MC simulations show that a slightly disordered AFM configuration is more stable at low temperatures (T=1K), which is in agreement with the collapse of the magnetization observed in the experiments at this phase transition, and with the first-principles studies of the phase stability. [9].

C. Stacking faults effects

In the mean-field approximation (MFA), one can estimate the ordering temperature as

$$T_{critical} = \frac{2J_0}{3k_B}, \quad (2)$$

where $J_0 = \sum_j J_{0j}$ corresponds to the sum of the exchange interaction energies [36]. For structures with stacking faults (such as the *Sm*-type structure), one may identify at least two sets of J_{ij} associated with either *hcp* or *fcc* sites. Thus, we can split

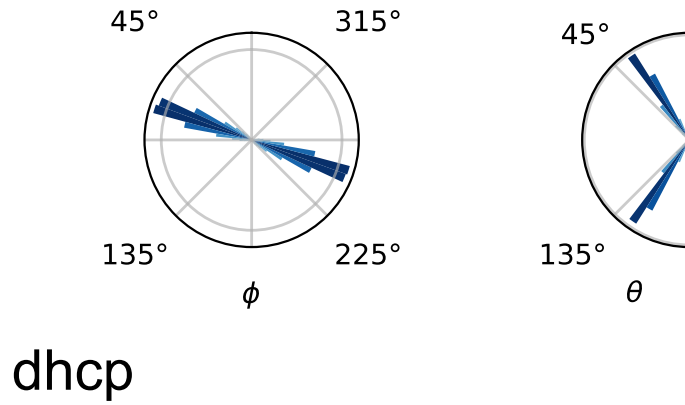
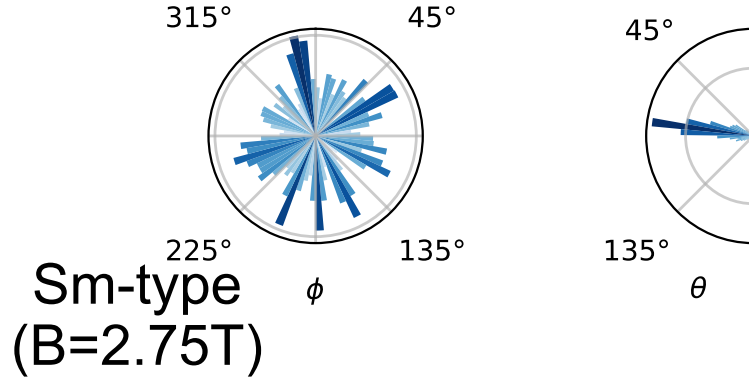
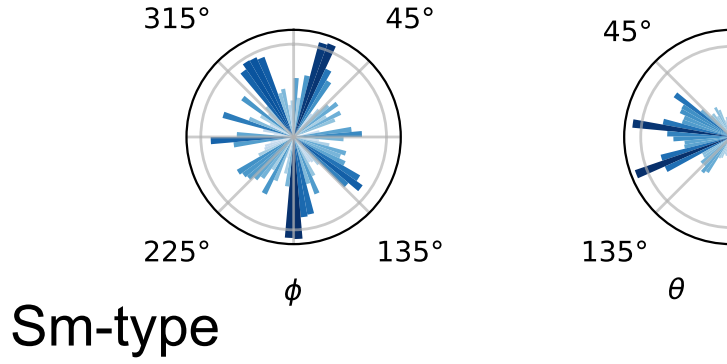


FIG. 4. Statistical distribution of spin directions (spherical coordinates with azimuthal angle ϕ in the x-y plane and polar angle θ) for different Gd systems simulated at T=1K with UppASD.

J_0 in Equation 4 in two terms, one containing the sum of all exchange interactions located in fcc sites, J_0^{fcc} , and the sum of all exchange interactions located in hcp sites, J_0^{hcp} . The two terms are summed, taking into account the fraction of the respective stacking environment, e.g., in the case of the Sm -type structure, which is composed of 2/3 of hcp sites and 1/3 fcc sites we use $J_0 = 0.6\bar{6}J_0^{hcp} + 0.3\bar{3}J_0^{fcc}$, which is then used in Equation 4 to estimate the ordering temperature.

Extending this idea to other stacking structures, we propose to evaluate J_0 as an average of both fcc and hcp environments, $J_0 = xJ_0^{hcp} + (1 - x)J_0^{fcc}$, with x being the ratio of the number of hcp layers in the structure. Applying this to Equation 4, we obtain a MFA model for $T_{critical}$ dependence on stacking faults:

$$\begin{aligned} T_{critical} &= \frac{2}{3k_B} \left(xJ_0^{hcp} + (1 - x)J_0^{fcc} \right) \\ &= xT_C^{hcp} + (1 - x)T_C^{fcc}. \end{aligned} \quad (3)$$

In the Supplement, we discuss further the applicability of this equation.

To be able to study the pressure dependence of the transition temperature based on Equation 3, we need a model that relates the fraction of hcp layers, x , and fcc layers, $(1 - x)$, to the applied pressure.

As an approximate description, we consider a linear decrease of x with pressure, with a different decrease ratio between the transition ranges (validity shown in Figure S.5 in the Supplement). Specifically, when transitioning from the hcp phase (where $x=1$ and is stable at $P=0$ GPa) to the Sm -type phase (where $x=2/3$ and is stable at $P=2$ GPa), the decrease ratio has one value, $1.\bar{6}$ stacks/GPa. When transitioning from the Sm -type phase to the $dhcp$ phase (where $x=1/2$ and is stable above $P=6.5$ GPa), a different decrease ratio is applicable, $0.\bar{037}$ stacks/GPa.

We used this relationship between pressure and the formation of stacking faults, combined with Equation 3 and the J_0^{hcp} and J_0^{fcc} calculated for the Sm -type structure, to evaluate the variation of $T_{critical}$ with pressure. Employing the J_{ij} obtained for the

Sm -type is motivated by the co-existence of both hcp and fcc sets in the phase and for being roughly the expected structure throughout the majority of the pressure range that was explored (0-6 GPa). The calculated $T_{critical}$ values are in good agreement with experimental findings reported in Reference [15], as shown in Figure 3.

Here, the agreement in the pressure range of the Sm -type structure (2-6.5 GPa) supports the hypothesis of the formation of fcc stacking faults under pressure as the primary mechanism for the $T_{critical}$ variation observed experimentally. The pressure change of the ordering temperature from a model that only considers a volume variation of a stacking-fault-free hcp phase is seen from Figure 3 to fail in reproducing the experimental trend, since the so obtained T_C barely changes with the pressure (blue circles).

In the region between 0-2 GPa, our model has a less accurate agreement with the experimental data, since it predicts a sharper decrease of $T_{critical}$ compared to the observed value. While the estimated trend aligns with the two experimental data points closest to $P=2$ GPa, the remaining data appears to be in better agreement with the results based solely on volumetric effects (depicted as blue circles in Figure 4). Intuitively, it sounds reasonable that the hcp structure would withstand some volume contraction before entering the regime of formation of fcc environments, which would imply a slower variation of $T_{critical}$ when $P \rightarrow 0$ in comparison to the linear approach employed in our model. We also attribute the fast $T_{critical}$ decline predicted at low pressures to the simplification made of not including pressure effects on the exchange parameters. In an ideal case, we expect that J_0^{hcp} and J_0^{fcc} vary in the intermediate structures. This effect has been neglected since we considered the values from the Sm -type structure which explains the difference between $T_{critical}$ from the model and the hcp phase at zero pressure. This difference makes it also evident how J_0^{hcp} is more susceptible to the formation of stacking faults than to volume effects (by comparison with hcp in different volumes).

Another consequence of taking fixed J_0^{hcp} and J_0^{fcc} values is the inability to predict the collapse of magnetic ordering near the transition to the *dhcp* phase. Theoretically, one could improve the model by calculating the J_{ij} parameters of intermediate structures between the *hcp*, the *Sm*-type and the *dhcp* phases. However, the unit cell needed would increase significantly in the number of atoms, rapidly raising the computational effort for the calculation of the exchange parameters.

In experimental reports, dT_C/dP was determined by linear regression of data points in the whole 0-6 GPa interval being obtained a range 10.6-17.2 K/GPa of values for dT_C/dP [10, 11, 14–16], i.e., the change in slope beyond 2 GPa was ignored. If the regression is done separately for the 0-2 GPa and 2-6 GPa regions, we obtain distinct slopes for the respective regions (see Figure S.6 in Supplement). This behaviour is in line with our hypothesis of the magnetism being critically coupled to the number of stacking faults, which should have different formation rates in these intervals.

An attempt to apply this model to describe the magnetization drop under pressure can be seen in the Supplement. Notably, the coexistence of distinct magnetic configurations in the phases (*hcp*, *Sm*-type, and *dhcp*) suggests that their interaction gives rise to an intricate magnetic arrangement. It becomes apparent that the experimental drop in magnetization cannot simply be explained by changes in local moments in the individual phases or simple changes in magnetic ordering. A more sophisticated approach which describes the interaction between the magnetic phases is necessary to accurately describe this phenomenon. In order to do so, measurements of the magnetic order of bulk Gd at different pressures would offer important clues for the theoretical modelling.

IV. CONCLUSIONS

In this work, we investigate the causes for the observed pressure-dependence of the magnetic properties of bulk Gd from first-principles calculations. As for other rare-earth elements, we observe that the exchange parameters depend on the stacking structure, with the appearance of additional AFM couplings for the *Sm*-type structure (*9R*) and *dhcp*. With this in mind, we describe with success the variation of the magnetic order-disorder temperature along the 0-6 GPa pressure range as linearly dependent on the formation of *fcc* stackings. By doing so, we identify two different $T_{critical}/P$ rates, as a consequence of the different stacking fault formation rates with the pressure associated with the *hcp* \rightarrow *Sm*-type transition and *Sm*-type \rightarrow *dhcp* transitions. Although this change in behaviour is not considered in previous reports, the experimental data show a similar shift in pressure dependence.

Despite the strong coupling between structure and magnetic properties observed, it was possible to describe the pressure dependence of the Curie temperature reasonably well, without considering the pressure-induced effects on the J_{ij} couplings. Moreover, we assume that in the case of phase coexistence, the interaction between phases can be simplified as an external magnetic field created by the respective magnetization. However, this approximation fails to explain the magnetization dependence on pressure and its collapse close to the transition to the *dhcp* structure. We link this failure to a more complex magnetic configuration resulting from the coexistence of phases with different magnetic ordering which leads to a competition between AFM and FM alignment of the spins.

V. ACKNOWLEDGMENTS

RMV would like to thank Anders Bergman for the discussion on magnetic frustrated configurations and Erna K. Delczeg-Czirjak for the support in validation calculations. This work was supported by the Swedish Foundation for Strategic Research, within the project Magnetic Materials for Green Energy Technology (ref. EM16-0039), StandUp, eSENCE, the Swedish Energy Agency (Energimyndigheten), The Knut and Alice Wallenberg Foundation, the Magnus Ehrnrooth Foundation, the ERC (FASTCORR project) and the Swedish Research Council (VR). The computations performed in this work were enabled by resources provided by the CSC – IT Center for Science, Finland, and by the Swedish National Infrastructure for Computing (SNIC) at NSC and PDC centres, partially funded by the Swedish Research Council through grant agreement no. 2018-05973.

VI. DECLARATION OF INTEREST STATEMENT

The authors declare that they have no known competing financial interests or personal relationships that could have appeared to influence the work reported in this paper.

-
- [1] K. A. Gschneidner and L. Eyring, *Handbook on the Physics and Chemistry of Rare Earths*, Vol. 1 (Elsevier, 1978).
 - [2] J. Jensen and A. R. Mackintosh, *Rare earth magnetism* (Clarendon Press Oxford, 1991).
 - [3] I. L. Locht, Y. O. Kvashnin, D. C. Rodrigues, M. Pereiro, A. Bergman, L. Bergqvist, A. I. Lichtenstein, M. I. Katsnelson, A. Delin, A. B. Klautau, B. Johansson,

- I. Di Marco, and O. Eriksson, Standard model of the rare earths analyzed from the Hubbard i approximation, *Physical Review B* **94**, 085137 (2016).
- [4] I. Turek, J. Kudrnovský, G. Bihlmayer, and S. Blügel, Ab initio theory of exchange interactions and the Curie temperature of bulk Gd, *Journal of Physics Condensed Matter* **15**, 2771 (2003).
- [5] L. M. Sandratskii and J. Kübler, Local Magnetic Moments of Conduction Electrons in Gadolinium, *Europhysics Letters* **23**, 661 (1993).
- [6] L. M. Sandratskii, Exchange splitting of surface and bulk electronic states in excited magnetic states of Gd: First-principles study, *Physical Review B* **90**, 184406 (2014).
- [7] M. Colarieti-Tosti, S. I. Simak, R. Ahuja, L. Nordström, O. Eriksson, D. Åberg, S. Edvardsson, and M. S. S. Brooks, Origin of Magnetic Anisotropy of Gd Metal, *Physical Review Letters* **91**, 157201 (2003).
- [8] R. M. Vieira, O. Eriksson, T. Björkman, A. Bergman, and H. C. Herper, Realistic first-principles calculations of the magnetocaloric effect: applications to hcp gd, *Materials Research Letters* **10**, 156 (2022).
- [9] Q. Li, H. Ehteshami, K. Munro, M. Marqués, M. I. McMahon, S. G. MacLeod, and G. J. Ackland, Nonexistence of the s-f volume-collapse transition in solid gadolinium at pressure, *Physical Review B* **104**, 144108 (2021).
- [10] N. Golosova, D. Kozlenko, E. Lukin, S. Kichanov, and B. Savenko, High pressure effects on the crystal and magnetic structure of 160Gd metal, *Journal of Magnetism and Magnetic Materials* **540**, 168485 (2021).
- [11] M. Mito, Y. Kimura, K. Yamakata, M. Ohkuma, H. Chayamichi, T. Tajiri, H. Deguchi, and M. Ishizuka, Relationship of magnetic ordering and crystal structure in the lanthanide ferromagnets Gd, Tb, Dy, and Ho at high pressures, *Physical Review B* **103**, 024444 (2021).

- [12] E. Mendive-Tapia and J. B. Staunton, Theory of Magnetic Ordering in the Heavy Rare Earths: Ab Initio Electronic Origin of Pair- and Four-Spin Interactions, *Physical Review Letters* **118**, 197202 (2017).
- [13] G. K. Samudrala, G. M. Tsoi, S. T. Weir, and Y. K. Vohra, Structural and magnetic phase transitions in gadolinium under high pressures and low temperatures, *High Pressure Research* **34**, 385 (2014).
- [14] D. D. Jackson, V. Malba, S. T. Weir, P. A. Baker, and Y. K. Vohra, High-pressure magnetic susceptibility experiments on the heavy lanthanides Gd, Tb, Dy, Ho, Er, and Tm, *Physical Review B* **71**, 184416 (2005).
- [15] M. Tokita, K. Zenmyo, H. Kubo, K. Takeda, M. Mito, and T. Iwamoto, RKKY interaction in metallic Gd in GPa pressure regions, *Journal of Magnetism and Magnetic Materials* **272-276**, 593 (2004).
- [16] T. Iwamoto, M. Mito, M. Hidaka, T. Kawae, and K. Takeda, Magnetic measurement of rare earth ferromagnet gadolinium under high pressure, *Physica B: Condensed Matter* **329-333**, 667 (2003).
- [17] D. B. McWhan and A. L. Stevens, Effect of Pressure on the Magnetic Properties and Crystal Structure of Gd, Tb, Dy, and Ho, *Physical Review* **139**, A682 (1965).
- [18] B. Coles, Transformation effects, stacking faults and magnetism in the light rare earths, *Journal of Magnetism and Magnetic Materials* **15-18**, 1225 (1980).
- [19] W. A. Grosshans and W. B. Holzapfel, Atomic volumes of rare-earth metals under pressures to 40 GPa and above, *Physical Review B* **45**, 5171 (1992).
- [20] J. M. Wills, O. Eriksson, P. Andersson, A. Delin, O. Grechnev, and M. Alouani, *Full-Potential Electronic Structure Method*, Springer Series in Solid-State Sciences, Vol. 167 (Springer Berlin Heidelberg, Berlin, Heidelberg, 2010).
- [21] J. P. Perdew and Y. Wang, Accurate and simple analytic representation of the electron-gas correlation energy, *Physical Review B* **45**, 13244 (1992).

- [22] T. Björkman, Cif2cell: Generating geometries for electronic structure programs, Computer Physics Communications **182**, 1183 (2011).
- [23] J. Korringa, On the calculation of the energy of a Bloch wave in a metal, Physica **13**, 392 (1947).
- [24] W. Kohn and N. Rostoker, Solution of the Schrödinger Equation in Periodic Lattices with an Application to Metallic Lithium, Physical Review **94**, 1111 (1954).
- [25] H. Ebert, D. Ködderitzsch, and J. Minár, Calculating condensed matter properties using the KKR-Green's function method - Recent developments and applications, Reports on Progress in Physics **74**, 96501 (2011).
- [26] P. Soven, Coherent-Potential Model of Substitutional Disordered Alloys, Physical Review **156**, 809 (1967).
- [27] G. M. Stocks, W. M. Temmerman, and B. L. Gyorffy, Complete Solution of the Korringa-Kohn-Rostoker Coherent-Potential-Approximation Equations: Cu-Ni Alloys, Physical Review Letters **41**, 339 (1978).
- [28] A. I. Liechtenstein, V. I. Anisimov, and J. Zaanen, Density-functional theory and strong interactions: Orbital ordering in Mott-Hubbard insulators, Physical Review B **52**, R5467 (1995).
- [29] Y. O. Kvashnin, R. Cardias, A. Szilva, I. Di Marco, M. I. Katsnelson, A. I. Lichtenstein, L. Nordström, A. B. Klautau, and O. Eriksson, Microscopic origin of Heisenberg and non-Heisenberg exchange interactions in ferromagnetic bcc Fe, Physical Review Letters **116**, 217202 (2015).
- [30] A. Liechtenstein, M. Katsnelson, V. Antropov, and V. Gubanov, Local spin density functional approach to the theory of exchange interactions in ferromagnetic metals and alloys, Journal of Magnetism and Magnetic Materials **67**, 65 (1987).
- [31] B. Skubic, J. Hellsvik, L. Nordström, and O. Eriksson, A method for atomistic spin dynamics simulations: implementation and examples, Journal of Physics: Condensed

Matter **20**, 315203 (2008).

- [32] O. Eriksson, A. Bergman, L. Bergqvist, and J. Hellsvik, *Atomistic Spin Dynamics*, Vol. 1 (Oxford University Press, Oxford, 2017).
- [33] E. Y. Tonkov, I. L. Aptekar, V. F. Degtareva, and Y. I. Krasavin, Conversion of the metastable high-pressure phase of Gd, Tb, Dy, and Ho into the stable phase, Sov. Phys.-Dokl.(Engl. Transl.);(United States) **21** (1976).
- [34] A. Nakaue, Studies on the pressure-temperature phase diagram of Nd, Sm, Gd and Dy, Journal of the Less Common Metals **60**, 47 (1978).
- [35] U. Kamber, A. Bergman, A. Eich, D. Iuşan, M. Steinbrecher, N. Hauptmann, L. Nordström, M. I. Katsnelson, D. Wegner, O. Eriksson, and A. A. Khajetoorians, Self-induced spin glass state in elemental and crystalline neodymium, Science **368**, eaay6757 (2020).
- [36] Y. O. Kvashnin, O. Grånäs, I. Di Marco, M. I. Katsnelson, A. I. Lichtenstein, and O. Eriksson, Exchange parameters of strongly correlated materials: Extraction from spin-polarized density functional theory plus dynamical mean-field theory, Physical Review B - Condensed Matter and Materials Physics **91**, 1 (2015).
- [37] F. D. Murnaghan, The Compressibility of Media under Extreme Pressures, Proc. Natl. Acad. Sci. **30**, 244 LP (1944).

SUPPLEMENT

A. Additional results

TABLE II. Summary of the structural and magnetic properties from the DFT calculations.

Phase	a (Å)	c/a	$\langle m_{site} \rangle$ (μ_B)	ΔE_0 (mRy/atom)	
				FP-LMTO	CPA-ASA-KKR
<i>hcp</i> (FM)	3.642	1.60	7.59	-	-
<i>Sm</i> -type					
AFM (<i>fcc</i> DLM)			-	-	2.44
AFM	3.618	14.43	7.49	0	1.53
FiM			7.49	0.01	1.59
FM			7.53	0.3	0
FM (<i>fcc</i> DLM)			-	-	3.08
<i>dhcp</i>					
FM	3.402	3.25	7.41	0	-
AFM			7.37	0.39	-

TABLE III. Density of states at the Fermi level vs. pressure (volume only) in the hcp structure of Gd.

Pressure (GPa)	D(ϵ_F)
(GPa)	mRy/states/atom
0	12.25
2	11.96
4	11.44
6	11.86
8	12.73

B. Mean-field approximation T_C

$$T_{critical} = \frac{2J_0}{3k_B}, \quad (4)$$

Note that Equation 4 is only valid for systems with one magnetic sub-lattice, while by identifying that *fcc* and *hcp* sites have different sets of J_{ij} we are recognizing two magnetic sub-lattices. In that case, the correct calculation of the MFA would require the calculation of the highest eigenvalue of the Heisenberg Hamiltonian (see main text). However, given that both *hcp* and *fcc* sites have the same coordination number for the closest neighbours and similar magnetic properties, Equation 4 should give a reasonable approximation. We compared both approaches for the *Sm*-like phase observing only minor changes in the results.

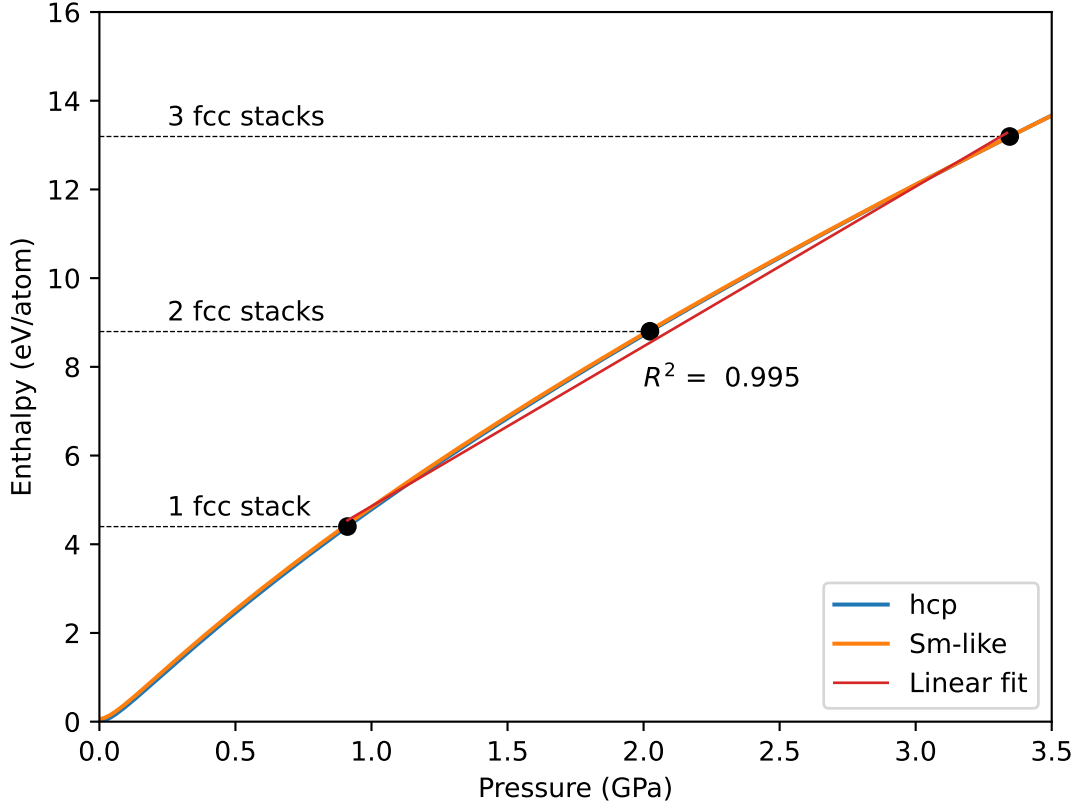


FIG. 5. Verification of linear assumption on the formation of stacking faults between $hcp \rightarrow Sm$ -like phases. Enthalpy calculated with the Murnaghan equation of state [37].

C. Magnetization

As discussed in the main text, the magnetic configurations of the hcp and Sm -type phases are very different. Here, we attempt to analyze the reduction of magnetization under pressure observed experimentally. Comparison of the local magnetic moments of different structures (see Table II) or for different volumes in the hcp phase shows minor variations, in agreement with previous studies [9]. Thus, the magnetization

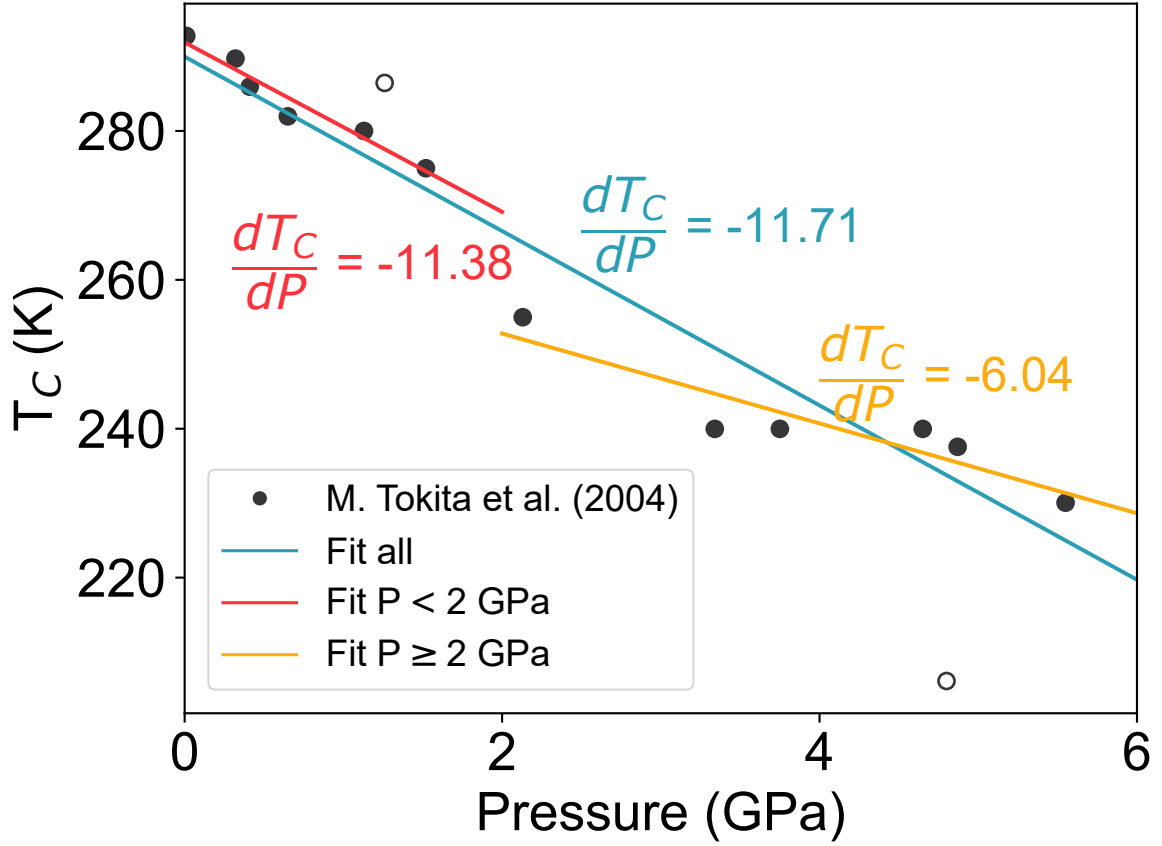


FIG. 6. Comparison of linear fits for different pressure intervals. The resultant dT_C/dP varies significantly if a different fit is made for the hcp and Sm-type phases.

variation must be related to changes in the magnetic ordering.

Whichever description of the $hcp \rightarrow Sm\text{-type} \rightarrow dhcp$ transition is used, either the spontaneous formation of the pressured phase followed by growth or accumulation of stacking faults, it implies the presence of at least two phases. Since the hcp and the Sm -type phase have very distinct magnetization, we tried to find the fraction (ρ) of hcp -phase at each pressure by fitting:

$$M_{expt}(P) = \rho M_{hcp}(T) + (1 - \rho) M_{Sm}(T) \quad (5)$$

to the magnetization-pressure data from Ref. [15]. As the temperature associated with the experimental data is unclear, we tried different temperatures in the range between 1-300 K using the magnetization from our Monte Carlo results. Unfortunately, the results obtained are not comparable with the estimation from volumetric analysis in Ref. [10], which predicts a fraction of *Sm*-type of about 65% at 2 GPa. In comparison, our closest value was 23%.

This disagreement shows that we cannot simply assume a coexistence of phases with static properties from the pure phases. Further, it suggests that it is necessary to consider pressure effects in the respective magnetization of the phases present. It is also important to note that the phases (*hcp*, *Sm*-like, and *dhcp*) have different magnetic configurations. In the case of coexistence, a more complex magnetic arrangement should arise from their interaction.